PROCEEDINGS B

royalsocietypublishing.org/journal/rspb

Research

Cite this article: Chou P-H *et al*. 2023 Cellular mechanisms underlying extraordinary sulfide tolerance in a crustacean holobiont from hydrothermal vents. *Proc. R. Soc. B* **290**: 20221973.
https://doi.org/10.1098/rspb.2022.1973

Received: 1 October 2022
Accepted: 17 November 2022

Subject Category:
Development and physiology

Subject Areas:
ecosystems, environmental science, physiology

Keywords:
shallow-water hydrothermal vent, sulfide detoxification, brachyuran crab, microbes, transporters, physiological adaptation

Author for correspondence:
Yung-Che Tseng
e-mail: yctseng@gate.sinica.edu.tw

†Equal contribution author.

Electronic supplementary material is available online at https://doi.org/10.6084/m9.figshare.c.6328044.

THE ROYAL SOCIETY PUBLISHING

Cellular mechanisms underlying extraordinary sulfide tolerance in a crustacean holobiont from hydrothermal vents

Pei-Hsuan Chou[1,†], Marian Y. Hu[2,†], Ying-Jey Guh[1], Guan-Chung Wu[3,4], Shan-Hua Yang[6], Kshitij Tandon[7], Yi-Ta Shao[5], Li-Yih Lin[9], Chi Chen[10], Kuang-Yu Tseng[11], Min-Chen Wang[1], Cheng-Mao Zhang[7], Bor-Cheng Han[12], Ching-Chun Lin[8], Sen-Lin Tang[7], Ming-Shiou Jeng[7], Ching-Fong Chang[4] and Yung-Che Tseng[1]

[1]Marine Research Station (MRS), Institute of Cellular and Organismic Biology, Academia Sinica, I-Lan County, Taiwan
[2]Institute of Physiology, Christian-Albrechts-University Kiel, Kiel, Germany
[3]Department of Aquaculture, National Taiwan Ocean University, Keelung, Taiwan
[4]Center of Excellence for the Oceans and [5]Institute of Marine Biology, National Taiwan Ocean University, Keelung, Taiwan
[6]Institute of Fisheries Science, National Taiwan University, Taipei City, Taiwan
[7]Biodiversity Research Center and [8]Biomedical Translation Research Center, Academia Sinica, Taipei City, Taiwan
[9]Department of Life Science, National Taiwan Normal University, Taipei City, Taiwan
[10]Doctoral Degree Program in Marine Biotechnology, National Taiwan Ocean University and Academia Sinica, Taipei City, Taiwan
[11]Department of Life Science, Tunghai University, Taichung, Taiwan
[12]School of Public Health, Taipei Medical College, Taipei, Taiwan

G-CW, 0000-0002-9520-9864; L-YL, 0000-0003-3353-4503; Y-CT, 0000-0001-7489-0403

The shallow-water hydrothermal vent system of Kueishan Island has been described as one of the world's most acidic and sulfide-rich marine habitats. The only recorded metazoan species living in the direct vicinity of the vents is *Xenograpsus testudinatus*, a brachyuran crab endemic to marine sulfide-rich vent systems. Despite the toxicity of hydrogen sulfide, *X. testudinatus* occupies an ecological niche in a sulfide-rich habitat, with the underlying detoxification mechanism remaining unknown. Using laboratory and field-based experiments, we characterized the gills of *X. testudinatus* that are the major site of sulfide detoxification. Here sulfide is oxidized to thiosulfate or bound to hypotaurine to generate the less toxic thiotaurine. Biochemical and molecular analyses demonstrated that the accumulation of thiosulfate and hypotaurine is mediated by the sodium-independent sulfate anion transporter (SLC26A11) and taurine transporter (Taut), which are expressed in gill epithelia. Histological and metagenomic analyses of gill tissues demonstrated a distinct bacterial signature dominated by *Epsilonproteobacteria*. Our results suggest that thiotaurine synthesized in gills is used by sulfide-oxidizing endo-symbiotic bacteria, creating an effective sulfide-buffering system. This work identified physiological mechanisms involving host-microbe interactions that support life of a metazoan in one of the most extreme environments on our planet.

1. Background

Hydrogen sulfide is highly toxic for organisms due to its ability to inhibit cytochrome-c oxidase, a critical enzyme for mitochondrial respiration [1]. Therefore, metazoans living in sulfide-rich waters like those found in most hydrothermal vent systems evolved behavioural, morphological and

physiological mechanisms to allow existence in these highly toxic marine habitats [2–6]. While some deep-sea hydrothermal vent species have sulfide detoxification mechanisms independent from microbial symbionts [7,8], many sessile species, including vesicomyid bivalves, mytilids and vestimentiferans, evolved symbioses with sulfide-oxidizing chemoautotrophic bacteria that support detoxification and provide nutrition to the host [9,10]. To date, many studies on sulfide detoxification mechanisms in marine species focused on those inhabiting deep-sea hydrothermal vent systems of the mid-ocean ridges [6,11]. However, volcanic vent systems can also be found in shallow waters that are among the most extreme marine habitats concerning sulfide toxicity. Shallow-water vent systems with moderate temperatures (<200°C), high concentrations of sulfide and CO_2 were abundant in the primeval oceans, but due to the decrease in volcanic activity, such vent systems became rare in today's oceans [12]. One of these vent systems is found off the coast of Taiwan in the shallow-water at the eastern part of Kueishan Island (24°50′N, 121°57′E) [13]. Kueishan Island lies to the southern rifting end of the Okinawa Trough, a back-arc depression of the Ryukyu arc-trench system and has active volcanic features [14]. This underwater volcano has been described as one of the world's most acidic vents, discharging water that has a high content of elemental sulfur particles, a minimum pH of 1.52 [15], and a gas composition consisting of high concentrations of sulfide (H_2S) (800 µM) and CO_2 (<92%) [13]. Due to these hostile conditions, the biodiversity of this vent habitat is extremely low [16], with the brachyuran crab *Xenograpsus testudinatus* being the only recorded metazoan species in the direct vicinity of the vents. *X. testudinatus* is endemic to shallow-water (<200 m) sulfide-rich vent systems [17], sporadically feeding on dead zooplankton killed by the toxic vent discharges [18].

Sulfide oxidation to the less toxic thiosulfate has been demonstrated as a major detoxification mechanism in other invertebrates from sulfide-rich marine habitats [7,8] that host sulfide-oxidizing endosymbionts in their tissues [19,20]. In addition, some hydrothermal vent species utilize sulfide-binding factors like hypotaurine that bind sulfide to synthesize thiotaurine, which is less toxic to cellular respiration [9,10]. These unusual amino acids were first discovered in vent vestimentiferans and bivalves that carry thiotrophic endosymbionts, but are also observed in species without endosymbionts. Accordingly, many invertebrates from vents and seeps have high concentrations of hypotaurine and thiotaurine independent from their symbioses with thiotrophic symbionts [10,21]. This adaptive sulfide detoxification mechanism is prevalent in animals that cannot avoid sulfide exposure (e.g. vestimentiferans, polychaetes, vesicomyid clams and bathymodiolin mussels) or that feed on external bacteria and detritus (e.g. polychaetes and gastropods) in sulfide-laden waters [9,10,19,22,23].

In most species, sulfide oxidation capacities are associated with specialized tissues, including the epidermis, gills and hepatopancreas [19,24–27]. In some vent species, these tissues exhibit distinct morphological features, including large numbers of electron-dense organelles termed sulfide oxidizing bodies [28]. Furthermore, sulfide-oxidizing endosymbionts are well known to be found in specialized tissues of vent species [29]. Vent-dwelling organisms like the sessile tubeworm *Riftia pachyptila* or some bivalve species have intracellular symbionts that are located in specialized host cells, the bacteriocytes of the trophosome or gill [30–32]. The host provides all substrates necessary for chemosynthesis to the symbionts [33], and in return, the symbionts provide fixed organic carbon to nourish the gutless host [34]. A recent study reported a specific microbial signature consisting of sulfur-oxidizing *Epsilonproteobacteria* and *Gammaproteobacteria* in several tissues of *X. testudinatus* [20,35]. *Epsilonproteobacteria* are capable of autotrophic growth fueled by oxidation of reduced sulfur compounds, and *Gammaproteobacteria* are known to perform chemolithoautotrophic sulfur oxidization [36–38]. However, it remains unknown if a specific microbial signature in *X. testudinatus* is associated with their high tolerance to environmental sulfide and if these microbial residents may provide nutrition to their hosts in this food-limited marine environment.

Thus, the present work aims at identifying and characterizing the cellular mechanisms of sulfide detoxification that allow *X. testudinatus* to exist in sulfide-rich vent systems. By determining and localizing the microbial community in gill tissues, the present work supports the concept that host–microbiome interactions underlie the extraordinary sulfide tolerance of *X. testudinatus*, allowing this species to occupy a unique ecological niche in one of the most extreme marine habitats.

2. Material and methods

(a) Study area and sample collection

Kueishan Island (121°57′ E; 24°50′N) is a volcanic island and the hydrothermal vents are only present near the eastern edge of Kueishan Island, including nine larger sulfur mounds and numerous smaller gas vents, distributed from the sublittoral to 20 m depth. The collection site (24°50.055′N; 121°57.716′E) is located at a cluster of vents discharging a sulfide-rich venting plume. Two perpendicular 100 m transect lines were set for the determination of sulfide gradients in this habitat. The north–south line was at a depth of 17 m, and the east–west line was at a depth descending from 6 to 19 m. The fieldwork was carried out from August 2005 to October 2019. Detailed information about field estimations and animal sampling is described in the electronic supplementary material.

(b) Determination of sulfur compounds

The procedure for measuring sulfide, sulfite and thiosulfate followed previously described protocols [39]. The reacted products were analysed using a Waters 600E HPLC (Mildford, MA, USA) within 2.5 h. And the sulfate concentration in SW and haemolymph was respectively determined with a portable photometer and 96-well plate photometer. Detailed information about sulfur compound determinations is described in the electronic supplementary material.

(c) Sulfide tolerance and exposure experiments

Tolerance of *X. testudinatus* and other marine species (including pebble crab (crabs), marine segmented worm (annelids), short-necked clam (molluscs), sea urchin (echinoderms) and sea bream (teleosts)) to environmental sulfide concentrations was investigated using a continuous flow-through system with dissolving rinsed $Na_2S{\cdot}9H_2O$ as described by [40]. Besides, *X. Testudinatus* was exposed to 1000 µM sulfide condition as described previously for 7 days. Detailed information treatment process is described in the electronic supplementary material.

(d) Hypotaurine and thiotaurine measurements

Hypotaurine and thiotaurine were extracted from haemolymph and norvaline was added as an internal standard. The sample

derivatives were injected in an ultra-performance liquid chromatography system (UPLC) (ACQUITY UPLC H-class System, Waters) equipped with a TUV detector and then identified and quantified by comparing sample data with retention times and peak areas of standards. Detailed information about hypotaurine and thiotaurine measurements is described in the electronic supplementary material.

(e) Purification of total RNA and reverse-transcription

Purification of total RNA and RT-PCR were performed as previously described [3]. Detailed information about molecular sample preparation is described in the electronic supplementary material.

(f) Molecular cloning

To amplify the partial cDNA fragment of SLC26A11 and Taut family genes, primers for *slc26a11* and *slc6a6* (encoded as Taut) were designed, as shown in electronic supplementary material, table S2. For PCR amplification, 1 µg of cDNA was used as a template. Detailed information about the cloning process is described in the electronic supplementary material.

(g) Quantitative real-time quantitative PCR

Primers of *slc26a11a*, *slc26a11b*, *taut1* and *taut2* genes were designed as listed in electronic supplementary material, table S2. Quantitative real-time quantitative PCR (qRT-PCR) was performed on a Roche LightCycler System (Roche Applied Science, Mannheim, Germany) using the LightCycler 480 SYBR Green I Master (Roche), and the ribosomal protein L9 (*rpl9*) was used as the reference gene. Detailed information about the qRT-PCR is described in the electronic supplementary material.

(h) Transmission electron microscope

The ultrathin sections (70 nm) were prepared from the 5th pair of gill arches and cut by Leica EM UC7, then mounted on nickel grids, and observed by a Tecnai G2 F20 S-TWIN field emission gun electron microscope (FEI Company, USA). Detailed information about the transmission electron microscope (TEM) process is described in the electronic supplementary material.

(i) Fluorescence *in situ* hybridization and immunohistochemical staining

Horizontal sections (10 µm; vertical to vascular) from the 5th pair of gill arches were collected on poly-L-lysine-coated slides for experiments. For target gene RNA labelling, isolated plasmids from the targeted clones were used to synthesize antisense and sense RNA probes. For the H&E staining, sections were stained with haematoxylin and eosin. For immunohistochemical staining, the primary antibody for Na^+/K^+-ATPase (NKA), H-300, was used. For microbial communities visualization, 4 µm paraffin sections were prepared as previously described [35]. The oligonucleotide probes targeting general Eubacteria 16S rRNA (EUB338) and thiotrophic symbiont (BangT-642) were utilized. Detailed information about the fluorescence in situ hybridization (FISH) and immunohistochemical staining is described in the electronic supplementary material.

(j) DNA extraction, amplicon sequencing, data analysis and microbiome quantification

DNA extraction was performed as previously described [35]. The DNA tagging PCR (5 cycles) using the total genomic DNA sample (from the 5th pair of gill arches) was used to tag the ends of 16S RNA gene V6-V8 amplicons. The operational taxonomic units (OTUs) were taxonomically classified according to the SILVA database. For the quantitative PCR assay, two primer sets were designed to target the *Epsilonproteobacteria* and *Gammaproteobacteria* (listed in electronic supplementary material, table S2). Detailed information about the microbiome analysis is described in the electronic supplementary material.

(k) Protein purification and western blot analyses

Protein extractions and western blot analyses were performed as previously described [3]. Detailed information about the protein expression analysis is described in the electronic supplementary material.

(l) Statistical analyses

Values are presented as the mean ± standard deviation (s.d.). Statistical analyses were performed using Sigma Stat 10.0 (Systat Software). Student's unpaired *t*-test was used to compare thiosulfate, hypotaurine and thiotaurine contents in haemolymph, RNA/protein expression in gill. One-way ANOVA followed by Tukey's *post-hoc* tests were used to compare thiosulfate contents in gills under different sulfide concentrations and the microbiome abundances in gills along with the time series. In all cases, significance was defined as $p < 0.05$.

3. Results and discussion

(a) Environmental sulfide concentrations of the shallow-water hydrothermal vent system and sulfide tolerance of *X. testudinatus*

The shallow-water (<25 m) hydrothermal vent system of Kueishan Island (24°50′N, 121°57′E) is located at the western edge of the Pacific Ocean, off the coast of Taiwan [13] (figure 1*a*; electronic supplementary material, video S1). *X. testudinatus* is the only metazoan species in the direct vicinity of the vents usually found at high densities within sulfur-covered crevices (figure 1*b* and *c*; electronic supplementary material, video S2). Based on our observations, *X. testudinatus* do not congregate near the vent fluid directly above the vent opening but rather in the surrounding area that is less impacted by the heat from the vents. It has been suggested that the extremely high and fluctuating sulfide concentrations are the major factor for the very low biodiversity of macrofauna in this habitat [41,42]. In the present study, water sulfide concentrations of the two main hydrothermal vent areas, Site 2 and Site 6, were determined to be 762.90 ± 8.52 µM and 786.40 ± 79.52 µM, respectively (figure 1*d*). These hydrogen sulfide concentrations exceed those measured in hydrothermal vent fields of the deep-sea that typically range from 6–318 µM [26,43–45]. Our most recent data also revealed that the sulfide concentrations in the vent areas where *X. testudinatus* congregated fluctuated dramatically [35] with peak sulfide levels higher than 1000 µM after a dramatic geological activity. The haemolymph of *X. testudinatus* specimens collected from this area contained high concentrations of sulfide derivatives, including sulfate and thiosulfate (figure 1*e*), indicating that *X. testudinatus* utilizes sulfide oxidation as a detoxification mechanism. The oxidation of sulfide to thiosulfate is a widespread detoxification mechanism and has been demonstrated for other crustaceans from sulfide-rich marine sediments [46,47] and deep-sea vent systems [26]. The evolutionary advantage of generating thiosulfate as a detoxification metabolite lies in

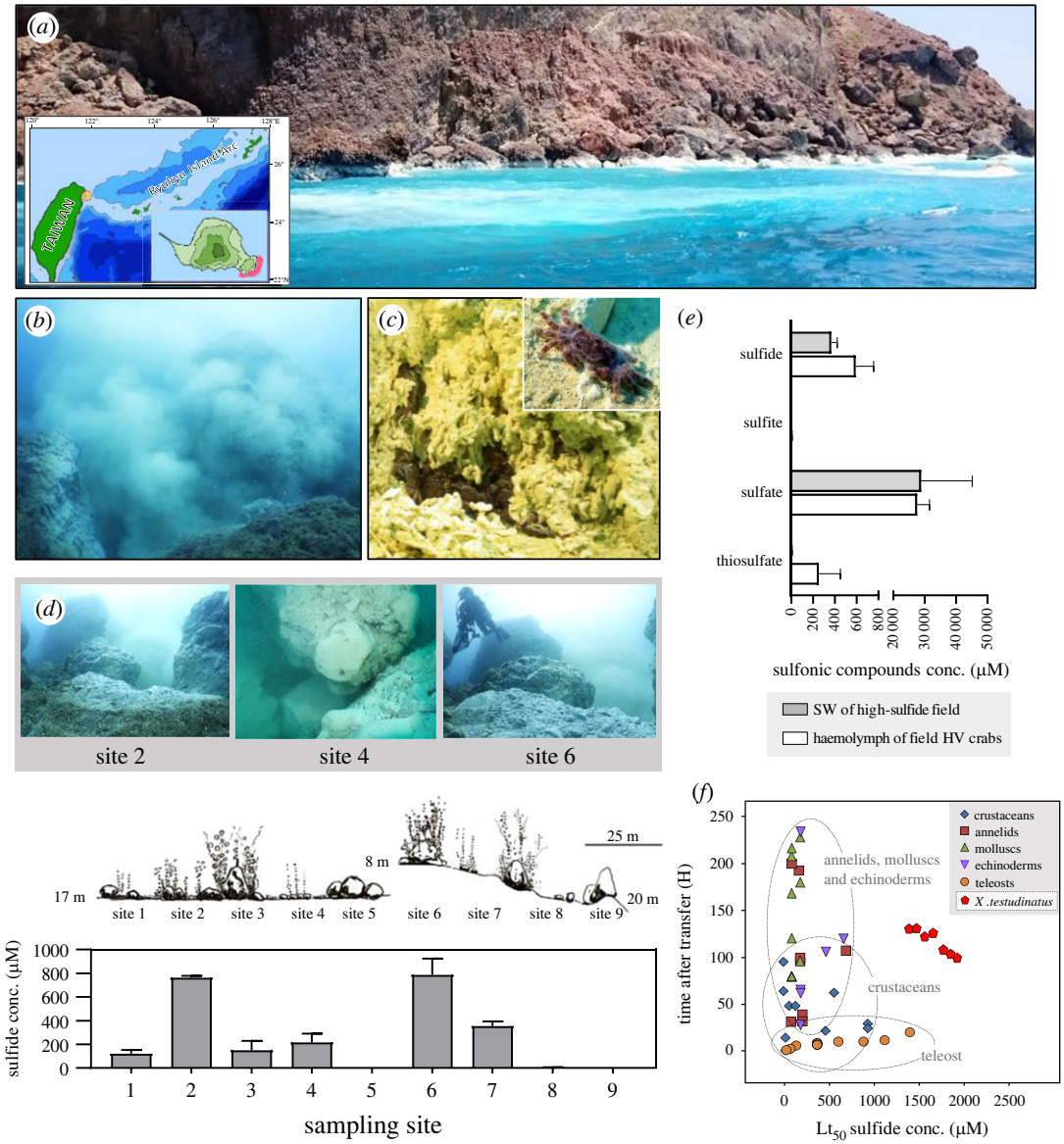

Figure 1. Landscape and physiochemical features of the hydrothermal vent system study area. (*a*) Picture of the surface seawater around the upper sublittoral hydrothermal vent region of the study site at Kueishan Island (24°50′N, 121°57′E). Kueishan Island lies at the southern rifting end of the Okinawa Trough (inserted panel). A large area of the sea surface has a white appearance because of sulfur particles from the volcanic vent discharge. (*b*) Underwater photographs of the vent system demonstrate the low abundance of metazoans in these sub-tropical waters. (*c*) A high density of *X. testudinatus* crabs which are endemic to sulfide-rich hydrothermal vent systems can be found in sulfide-rich crevices in the immediate vicinity of the vents. Active feeding behaviour can be observed where crabs scavenge sulfide-rich sediments and dead zooplankton that were killed by the toxic vent discharge. (*d*) sulfide concentrations were measured along two transects in the hydrothermal vent area of Kueishan Island. The schematic illustration shows the seafloor properties at the two sampling transects. The first transect included sampling sites 1–5 and was oriented in the north–south direction at 17 m depth. The second transect included sampling sites 6–9 with an east–west orientation and descended from 8 m to 20 m depth. Values are presented as mean ± s.d. ($n = 4$). (*e*) Content of sulfur compounds was measured in the seawater (SW) near Kueishan island (open bars) and the haemolymph of the native *X. testudinatus* (filled bars). Values represent the means ± s.d. ($n = 3$–7). (*f*) Sulfide tolerance as a function of exposure time of *X. testudinatus* (determined in the present study) compared to other marine species.

the fact that it has a more efficient stoichiometry than the synthesis of other sulfide derivates where 1 mol sulfide can be oxidized to thiosulfate with 1.5 mol oxygen [48].

Since *X. testudinatus* is the only recorded metazoan species reported in this shallow-water hydrothermal vent system, it can be expected to exhibit an extraordinary sulfide tolerance compared to other marine invertebrates. The median lethal time (Lt_{50}) of adult *X. testudinatus* exposed to up to 2000 µM sulfide at normoxic conditions was about 120 h which is high compared to other marine species, including organisms from other hydrothermal vent systems (figure 1*f*). The Lt_{50} value determined for *X. testudinatus* is higher than those of other hydrothermal vent species including the nematode *Oncholaimus campylocercoides* (108 h hypoxia and 500 µM sulfide [8]) and the annelid *Capitella capitata* (107 h hypoxia and 760 µM sulfide; [7]) (figure 1*f*); moreover, *X. testudinatus* appears to be more tolerant to sulfide than mactrid clams (*Mulinia lateralis*) that burrow into sediments containing sulfide concentrations that are lethal for most aquatic organisms [49]. *X. testudinatus* has substantial sulfide tolerance that is comparable to that of other vent crustaceans like the hydrothermal vent crab *Bythograea thermydron*. *Bythograea thermydron* has been demonstrated to have comparatively high sulfide tolerance with unchanged heart rates up to a sulfide concentration of 1400 µM [26]. Despite this high sulfide tolerance and a sulfide oxidation mechanism in place, little information is available regarding the cellular and molecular mechanisms of sulfide/thiosulfate

handling in *X. testudinatus* and other deep-sea hydrothermal vent crustaceans [26].

(b) Gill tissues and the hepatopancreas are major sites of sulfide detoxification

The gill organ of *X. testudinatus* consists of seven pairs of gill arches located within the branchial chamber (figure 2*a*) and represents together with the hepatopancreas, the major sites for sulfide detoxification indicated by high levels of thiosulfate (electronic supplementary material, figure S1). Animals collected from their natural habitats and those experimentally exposed to 1000 µM sulfide for 7 days exhibited a high thiosulfate concentration in these tissues and in the haemolymph. This suggests that these molecules are generated in the gills and the hepatopancreas and transported within the organism (figure 2*b*). Furthermore, hypotaurine and thiotaurine concentrations were measured in the haemolymph and gill tissues of *X. testudinatus*, and both amino acids were present in high concentrations in animals that were directly sampled from the native sulfidic environment (figure 2*c*). Some deep-sea vent vesicomyid bivalves, mytilids and vestimentiferans were shown to utilize such sulfide-binding compounds to decrease the potential affinity between sulfide and mitochondrial cytochrome c oxidase [23]. Hypotaurine, the precursor of taurine, is one such sulfide-binding compound. Upon sulfide binding, hypotaurine is converted to thiotaurine, which is less detrimental to cellular respiration. At vents and seeps, many invertebrates with or without thiotrophic symbionts have high levels of hypotaurine and thiotaurine [10,21]. This adaptation is prevalent in animals that are sessile and that cannot avoid sulfide exposure (e.g. vestimentiferans, polychaetes, vesicomyid clams and bathymodiolin mussels) or those that feed on external bacteria and detritus (e.g. polychaetes and gastropods) in sulfide-laden waters [9,10,19,22,23]. The present findings are also consistent with previous laboratory studies demonstrating that thiotaurine content increased during sulfide exposure of symbiont-bearing tissues (e.g. gills or foot) of deep-sea clams (vesicomyid), mussels (bathymodiolins), tube worms (vestimentiferans) [23] and shallow-living solemyid clams [50]. Although thiotaurine serves as a biomarker for deep-sea hydrothermal vent species [9], this is the first report that this molecule was detected in a crustacean species associated with sulfide detoxification mechanisms [51].

(c) Sulfate and taurine transporters are stimulated in gill tissues during exposure to sulfide

Our transcriptomic and gene expression analyses identified the sodium-independent sulfate anion transporters (*slc26a11a* and *slc26a11b*) as well as the taurine transporter (*taut2*) that are expressed in gill tissues at a relatively high level (figure 2*d*). sulfide exposure stimulated expression levels of these sodium-independent sulfate anion transporters (figure 2*e*,*g*; electronic supplementary material, figure S2). In live-bearing *Poecilia mexicana* fish collected from river drainage, *slc26a11* was associated with H_2S tolerance in a population living near a sulfide spring [27]. In *X. testudinatus* the sulfate and taurine transporters were mainly expressed in epithelial principal and pilaster cells (figure 2*f*,*h*), with particularly high expression of SLC26A11 homologues in the 3rd, 5th, 6th and 7th pairs of gill arches. Na^+/K^+-ATPase (NKA)-rich cells of the posterior gills are the major sites for ion- and pH regulatory capacities [3,52], and indicates that *X. testudinatus* also utilizes NKA-rich cells of posterior gills for the shuttling of sulfide derivates and detoxification. These observations suggest that the SLC26A11 sulfate anion transporter plays a pivotal role in the sulfide/sulfate metabolism of animals including those from hydrothermal vent systems.

Regulation of hypotaurine transport across the cell membrane depends on the taurine transporter (Taut) SLC6A6 [53,54], which couples sodium and chloride transport with that of taurine and hypotaurine [55]. We found that *X. testudinatus* had high expression levels of *taut2* in gill tissues (figure 2*d*) which is in accordance with observations made in the vent-endemic mussel *Bathymodiolus septemdierum* that also has particularly high expression levels of Taut in gill and gonad tissues [55]. Expression levels of Taut2 in gills of *X. testudinaus* were elevated in animals collected from the native sulfide-rich environment (figure 2*i*; electronic supplementary material, figure S2) compared to those kept under sulfide-free conditions. Furthermore, histological analyses using fluorescence *in situ* hybridization in posterior gills revealed that the *t*aut2 mRNA signal is co-expressed with NKA-rich principal and pilaster cells (figure 2*j*). This colocalization pattern suggests that *X. testudinatus* may use the electrochemical sodium gradient generated by the NKA to energize cellular hypotaurine accumulation for the detoxification of sulfide to thiotaurine. Notably, increased *slc26a11* and *slc6a6* mRNA expression levels do not perfectly mirror statistically higher protein levels in this study. However, higher mRNA levels of these transporters under high sulfide conditions correlate with the accumulation of their putative substrates, which could still promote transporter activity and influence turnover rate through posttranslational modifications.

(d) Structure of the gill microbiome depends on environmental sulfide concentrations

Thiotaurine has been proposed to play a dual role in vent-dwelling organisms. On one hand, it is used to detoxify sulfide compounds, and on the other hand, it can be used as an energy source by symbiotic sulfide-oxidizing bacteria [56]. Synthesis of thiotaurine from hypotaurine has been proposed to serve as a reversible non-toxic mechanism for sulfide storage in cells that can fuel endosymbionts during reduced sulfide availability [10]. For example, marine chemoautotrophic bacteria (e.g. *Beggiatoa* sp.) use sulfide and other reduced sulfur compounds for carbon fixation, with energetic efficiencies of 21–37% [57,58]. Furthermore, symbiotic sulfide-oxidizing bacteria have been shown to generate a large fraction of the energy requirements of their metazoan hosts in sulfidic habitats [59]. The present work, as well as a previous study [20], demonstrated a high abundance of *Epsilonproteobacteria* and *Gammaproteobacteria* within gill tissues of *X. testudinatus* crabs (figure 3, electronic supplementary material, figure S3). *Epsilonproteobacteria* are capable of autotrophic growth fueled by oxidation of reduced sulfur compounds, and *Gammaproteobacteria* are known to perform chemolithoautotrophic sulfur oxidization [36–38]. TEM (figure 3*a–e*) and fluorescence *in situ* hybridization (FISH) (figure 3*f*,*h*) analyses indicate the presence of symbiotic bacteria within gill tissues (figure 3*g*) of *X. testudinatus*. The symbiotic bacteria are not found on the surface of gill filaments/lamella but are located within epithelial cells

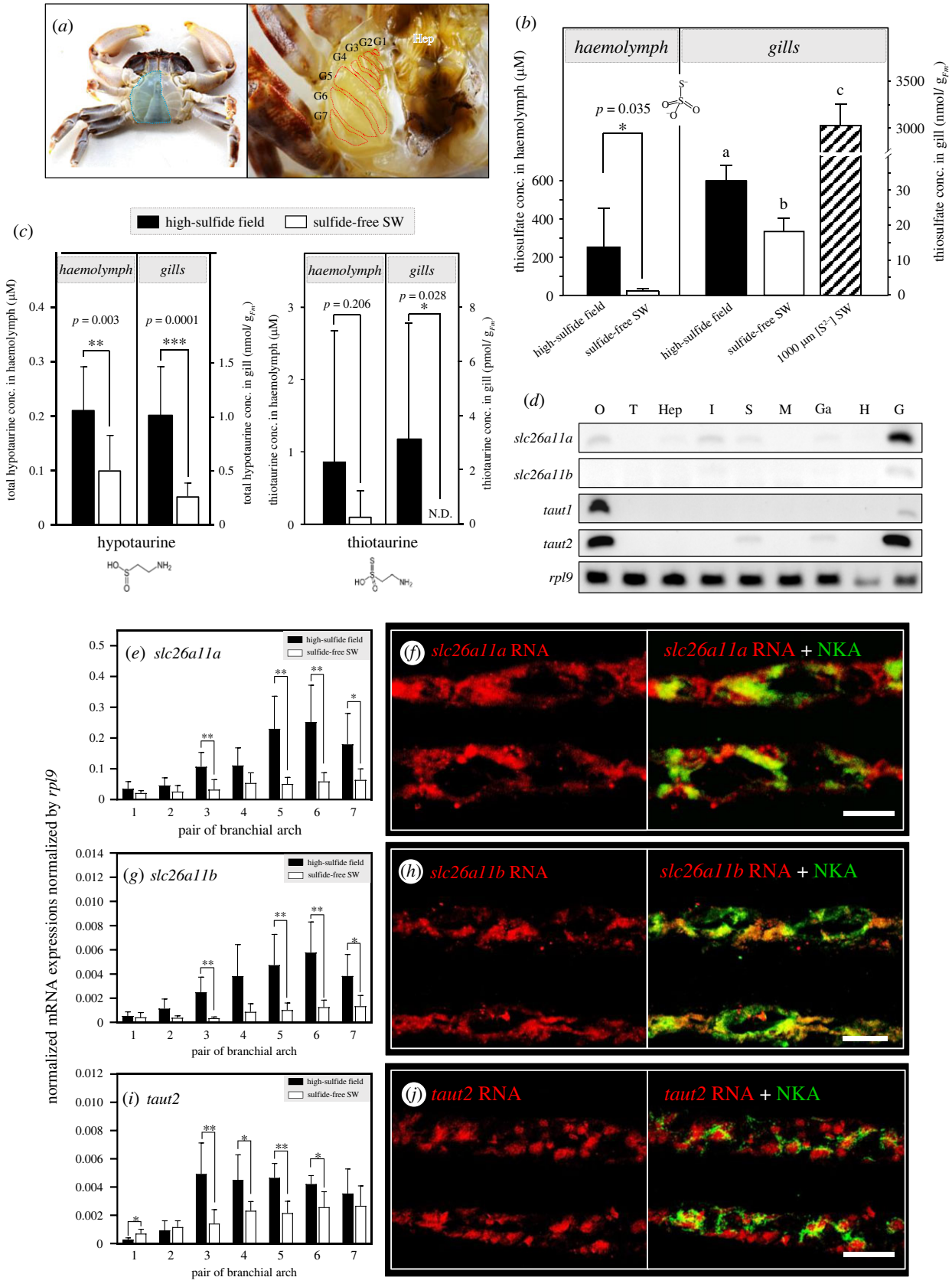

Figure 2. (*Caption overleaf.*)

(electronic supplementary material, figure S4). Ultrastructural analyses indicate the presence of coccoid-like symbiotic bacteria underlying the apical microvilli within principal cells of the gill (figure 3*a–c*). In addition, bacillus-like symbiotic bacteria clusters were observed in epithelial pilaster cell (figure 3*d*,*e*). Under fluorescence excitation light, crossed-sectioned gill tissue targeted with probes for bacteria (EUB338) displayed strong fluorescent signals within epithelial principal- and pilaster cells (figure 3*f*), suggesting the presence of endosymbionts within branchial cells. The morphology and tissue localization of microbial symbionts resemble those found in gill tissues of mytilid species from hydrothermal vent habitats [32]. In these bivalve species, coexistence of different bacteria species within one

Figure 2. (*Overleaf.*) Thiosulfate, hypotaurine and thiotaurine content and related transporter expression levels in *X. testudinatus* gill tissues. (*a*) Morphology of the branchial chamber of *X. testudinatus*. *X. testudinatus* has eight thoracic sternal segments and seven-gill pairs (aside to the hepatopacrease (Hep)) of which gill 1–3 (G1 to G3) are podobranchs, and G4 to G7 are arthrobranchs. (*b*) Thiosulfate contents were analysed in the haemolymph of *X. testudinatus* collected from the native high-sulfide field (black bar; $n = 4$), and sulfide-free SW acclimated counterpart (white bar; $n = 5$) (left panel). Whole gill tissue of *X. testudinatus* sampled from the high-sulfide field (black bar; $n = 8$), sulfide-free SW (white bar; $n = 8$), and 1000 µM [S^{2-}] SW (slashed bar; $n = 7$) were used for thiosulfate concentration measurements (right panel). (*c*) Hypotaurine (left panel) and thiotaurine (right panel) contents were analysed in the haemolymph of *X. testudinatus* collected from the high-sulfide field (black bar), and sulfide-free SW acclimated counterparts (white bar). (N.D. represents non-detected; $n = 10$). Due to the distinction between haemolymph and gill sample types, the representative value units for the contents on the *y*-axis of panels (*b*) and (*c*) were displayed in different formats. (*d*) Semi-quantitative RT-PCR analysis of the solute carrier family (SLC) 26 member 11 (*slc26a11a* and *slc26a11b*) and solute carrier family (SLC) 6 member 6 (*taut1* and *taut2*), was performed in gill (G), heart (H), ganglion (Ga), muscle (M), stomach (S), intestine (I), hepatopancreas (Hep), testis (T) and ovary (O) tissues of *X. testudinatus*. Ribosomal protein L9 (*rpl9*) was used as the internal control. Relative mRNA expression of *slc26a11a* (*e*) *slc26a11b* (*g*) and *taut2* (*i*) among different pairs of gill arch under the native high-sulfide hydrothermal vent environment (black bar) and sulfide-free SW (white bar). mRNA expression of the candidate genes was normalized to the mean value from ribosomal protein L9 (*rpl9*) ($n = 4$–6). Values are expressed as mean ± s.d. *, Significant differences between high-sulfide and sulfide-free conditions. (Student's *t*-test, *: $p < 0.05$, **: $p < 0.01$, ***: $p < 0.001$). Different letters indicate significant differences among different treatment groups (one-way ANOVA, Tukey's pairwise comparisons). The same horizontal gill section (the 5th pair of gill arch) of *X. testudinatus* was double-labelled with (*f*) *slc26a11a*-specific, (*h*) *slc26a11b*-specific or (*j*) *taut2*-specific RNA probe for fluorescence *in situ* hybridization (red signal) and Na^+/K^+ ATPase (NKA, green signal) antibody for immunohistochemical staining. Scale bars correspond to 10 µm.

bacteriocyte was demonstrated [32]. Interestingly, it seems that *X. testudinatus* maintains different endosymbionts within at least two cell types of the gill, including principal cells that face the seawater as well as pilaster cells that are in contact with the haemolymph.

In the next step, 16s rRNA analyses were used to investigate the temporal differences in gill tissue microbial community structure between crabs living in the native sulfide-rich vent system and those kept under sulfide-free conditions. Beta-diversity analysis using nMDS with Bray–Curtis similarities identified a distinct commensal bacteria community composition after transferring *X. testudinatus* from the high-sulfide field to sulfide-free seawater in the laboratory (figure 3*i*). Significance of clustering was tested with ANOSIM ($R = 0.846$, $p < 0.05$). *Epsilonproteobacteria* were the most dominant bacterial class from the phylum *Proteobacteria*, accounting for 34.79% to 89.31% of total sequences in the gills of *X. testudinatus* from native sulfide-rich vent systems (six independent samples) (figure 3*j*). This result is similar to a previous report where 16S rRNA gene amplicon pyrosequencing and full-length LoopSeq sequencing using tissues from *X. testudinatus* demonstrated the presence *Gamma-* and *Epsilonproteobacteria*that are usually associated with deep-sea hydrothermal systems [20,35,60,61]. Furthermore, the identified bacteria species are capable of autotrophic growth by oxidizing reduced sulfur compounds and a potential trophic symbiotic relationship was suggested [20,35]. Interestingly, after transfer from the native sulfide-rich vent system to the sulfide-free conditions for 72 h (five independent samples), *Gammaproteobacteria* became the most abundant class (14.27–42.33%) in gills. Crabs acclimated to sulfide-free seawater for two months had *Gammaproteobacteria* (10.62–49.20%) and *Alphaproteobacteria* (31.22–65.53%) as their dominantly associated bacterial classes with a relatively low fraction of *Epsilonproteobacteria* (0.04–3.88%) (figure 3*j*). Despite not reaching statistical significance due to a large degree of variation in the data, the alpha diversity analysis revealed that the microbial communities in the 5th pair of gill arches from the native sulfide-rich vent had lower microbial diversity ($p = 0.086$) and evenness ($p = 0.170$) than the samples from the acute 72 h sulfide-free treatment (figure 3*k*). When compared to 72 h of acute sulfide-free treatment, two months of exposure to sulfide-free SW resulted in a decrease in Shannon diversity index ($p = 0.086$) and evenness ($p = 0.110$) (figure 3*k*). In animals from the native sulfide-rich environment, the dominant groups within the proteobacteria classes were sulfur oxidizers, including *Sulfurovum* and *Thiotrichaceae*. After transfer to sulfide-free conditions, the relative abundance of *Sulfurovum* and *Thiotrichaceae* was decreased, with *Vibrionaceae* and *Pseudoalteromonas* becoming more dominant bacterial groups (electronic supplementary material, figure S3), which were described as potential symbiotic or pathogenic bacteria groups in aquatic organisms [62–64]. The relative expression levels of V6 to V8 hypervariable regions of *Epsilonproteobacteria* and *Gammaproteobacteria*, the key chemolithotrophic sulfur-oxidizing bacteria (SOB) at the deep-sea hydrothermal vent systems [65,66], 16S rRNA in the 5th pair of gill arch were further examined along a time course from several hours up to four months. We observed a decrease in 16S rRNA gene copy numbers for both *Epsilonproteobacteria* and *Gammaproteobacteria* at 6 h after transfer of the crabs from the native sulfide-rich vent system to sulfide-free conditions (electronic supplementary material, figure S5). After acclimation to sulfide-free seawater for more than 4 months, *Epsilonproteobacteria* were not detected in the 5th pair of gills, whereas *Gammaproteobacteria* relative abundance remained constant (figure 3*j*; electronic supplementary material, figure S5). FISH images utilizing a specific probe for thiotrophic symbionts further confirmed the absence of SOBs in gill epithelial cells (figure 3*h*). These findings further support the potential role of gill-associated microbial symbionts in handling sulfide and its metabolites in gill tissues of *X. testudinatus*. Based on our microbiome analyses and biochemical examination of sulfur compounds in gill tissues and/or haemolymph, we propose that the endosymbiotic bacteria in gills of *X. testudinatus* contribute to the breakdown of thiotaurine synthesized by the host. As such, reduced sulfur from the host cells could be used by the symbiotic bacteria as an energy source and in turn may provide the host with energy equivalents (summarized in figure 4). We cannot exclude the possibility that the gill microbiome is also affected by other environmental factors including pH and CO_2. However, the strongest changes in abundance were detected for sulfide metabolizing microbial residents upon transfer from the native field to sulfide-free conditions suggesting that sulfide is the major factor for the differences observed in the microbial composition of the

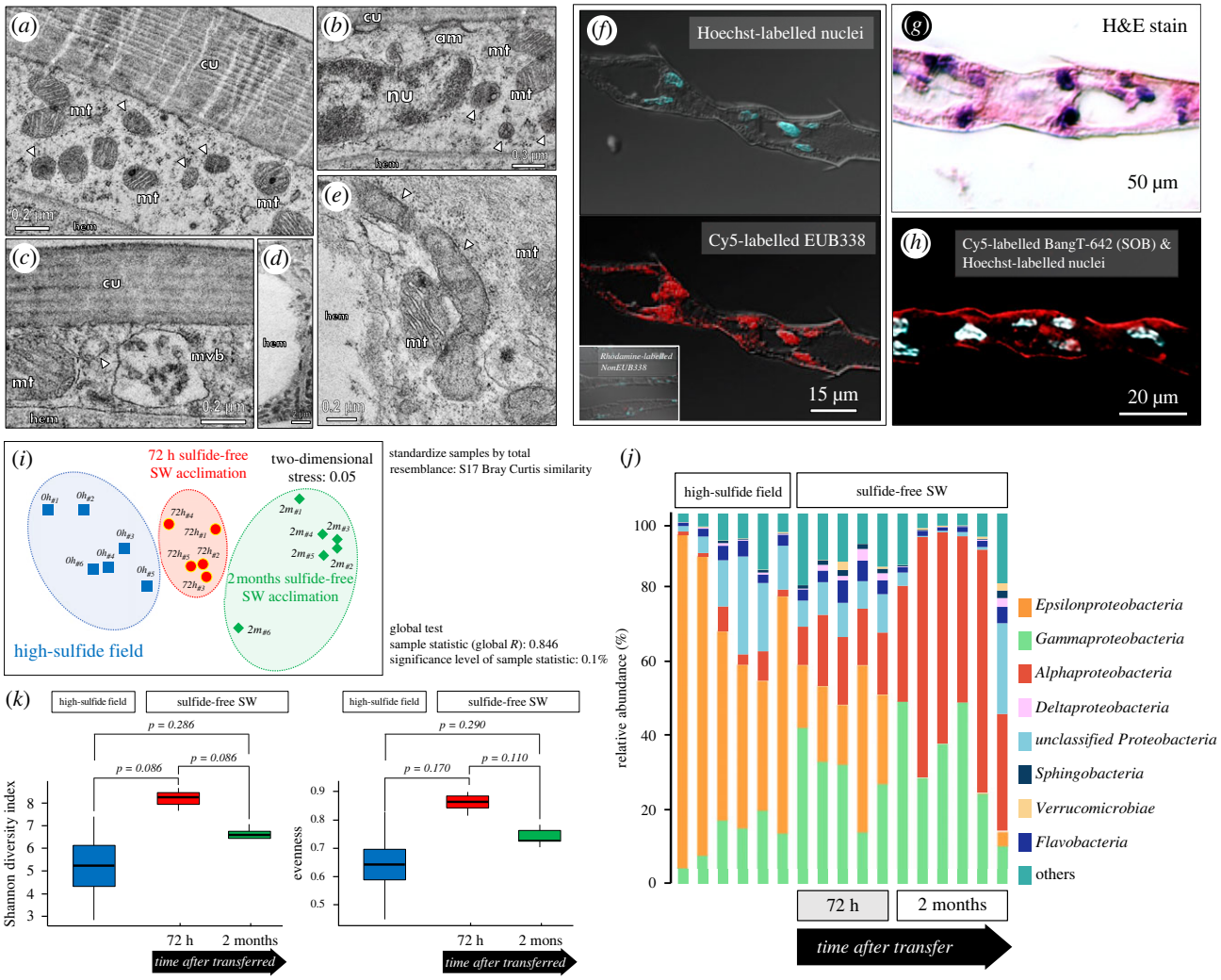

Figure 3. Analysis of the microbial community in gill tissues of *X. testudinatus*. (*a*) Distinct spatial organization of bacteria in transmission electron micrographs of the 5th pair gill arch. (*a–c*) Principal cells contain intracellular coccoid-like symbiotic bacteria (indicated by arrowheads) underlying the apical microvilli (am)-anchored cuticle (cu). Principal cells display typical subcellular structures including nuclei (nu), multiple mitochondria (mt), and multivascular body (mvb). (*d,e*) Intracellular image of the epithelial pilaster cell with bacillus-like symbiotic bacteria clusters (indicated by arrowheads). (*f–h*) Fluorescence *in situ* hybridization (FISH) on gill cross-sections (H&E staining in (*g*)) using a domain-specific probe (Cy5-labelled EUB338) for bacteria and a Rhodamine-labelled NonEUB338 probe to the adjacent section as the negative control (*f*). A specific probe for sulfur-oxidizing bacteria (Cy5-labelled BangT-642) was also applied on another gill cross-section (*h*). (*i,j*) Two-dimensional scatter plot shows multidimensional scaling (MDS) analysis (*i*), and relative abundance of major bacterial classes normalized to the total bacterial community (*j*). Gills of *X. testudinatus* from the high-sulfide field (blue squares), 72 h sulfide-free SW acclimation (red circles), and two months sulfide-free SW-acclimation (green diamonds) were used in the experiment. The similarity index was calculated using the relative percentage of each bacteria genus in each sample. (*k*) Alpha diversity (intra- host diversity) was assessed by describing and comparing the microbial biodiversity metrics. The Shannon diversity index and evenness were presented for the high-sulfide field, 72 h sulfide-free SW acclimation, and two months of sulfide-free SW-acclimation, and compared using a pairwise wilcox test.

gills. Furthermore, very different microbial signatures were documented for organisms from sulfide-rich hydrothermal vent systems and CO_2-enriched habitats [67,68]. This further underlines our conclusion that changes in the microbial signature of *X. testudinatus* observed in this work are predominantly related to environmental sulfide.

4. Conclusion and perspectives

In the shallow-water hydrothermal vent ecosystem of Kueishan Island, weak predator–prey relationships and low trophic complexity were observed. This is mostly because of the low species variety in this extreme and nutrient-poor vent habitat, which results in the sporadic feeding behaviour of *X. testudinatus* on marine snow [69]. This work provides a line of evidence demonstrating that the shallow-water hydrothermal vent crab, *X. testudinatus*, has evolved biochemical and cellular pathways of sulfide detoxification mechanisms associated with endo-symbiotic bacteria in their gill tissues. Understanding inter-kingdom interactions in ancient marine vent systems require understanding the sulfide-transport and -binding detoxifying processes by which the metazoan host interacts with endosymbiotic bacteria in sulfide-rich vent habitats. This is of particular significance given that hydrothermal vent systems are regarded to be the cradle of life on Earth [70] and hence may provide insight into the origins of host–microbe interactions [71]. Metabolic substrates generated by symbiotic bacteria or the bacteria itself may provide important additional energy sources for this crab population (figure 4). This trophic interaction between host and microbes in crustacean holobionts may explain the high concentration of (n-7) monounsaturated

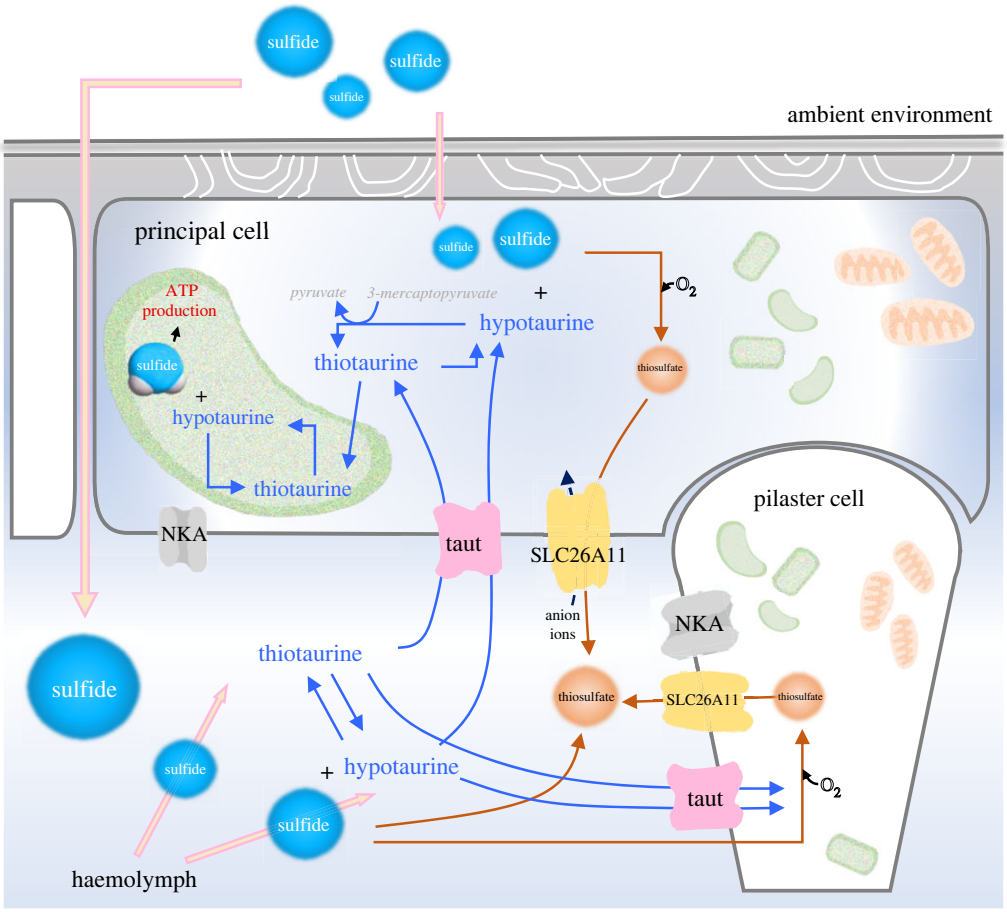

Figure 4. Putative organization of sulfur metabolite exchange and chemoautotrophic symbiotic relationship in gills of *X. testudinatus*. Reduced sulfur compounds (thiosulfate or sulfate), and sulfide-binding amino acid (hyprotaurine) are generated from sulfide and transported by SLC26A11 and Taut to minimize sulfide accumulation in the haemolymph. In gill epithelial cells, hypotaurine reacts with diffused sulfide to form thiotaurine. Thiotaurine and reduced sulfur compounds (including thiosulfate) may thereafter be translocated to the sulfur-reducing bacteria, where they can be further oxidized to yield ATP and reduced metabolites. ATP and reduced metabolites may then be used in part to drive net CO_2 fixation. Some fraction of the reduced carbon compounds synthesized by bacteria may be translocated to the animal host. The mitochondria and bacteria were shown in orange and green, respectively. Na^+/K^+-ATPase, NKA; SLC26A11, solute carrier family 26 member 11; Taut, taurine transporter.

fatty acids (MUFAs) in midgut tissues of *X. testudinatus* [72]. (n-7) MUFAs serve as trophic markers of bacterial origin and dominate the fatty acid profiles of many deep-sea hydrothermal vent species [73,74]. Accordingly, this work provides the first understanding of the cellular detoxification processes and physiology of host-microbe interactions that allowed a crustacean holobiont to thrive in ecological niches of the most extreme environments on our planet.

Data accessibility. The data that support the findings of this study are available in the electronic supplementary material [75].

Authors' contributions. P.-H.C.: data curation, investigation, resources, writing—original draft; M.Y.H.: data curation, investigation, methodology, writing—original draft, writing—review and editing; Y.-J.G.: data curation, investigation, methodology, writing—original draft; G.-C.W.: data curation, investigation, project administration, writing—original draft; S.-H.Y.: data curation, investigation, methodology, writing—original draft; K.T.: data curation, methodology; Y.-T.S.: data curation, investigation, resources; L.-Y.L.: data curation, investigation; C.C.: methodology, resources; K.-Y.T.: data curation, methodology; M.-C.W.: data curation, investigation, methodology, resources; C.-M.Z.: data curation, investigation, resources; B.-C.H.: data curation, methodology; C.-C.L.: data curation, methodology; S.-L.T.: data curation, investigation, methodology, supervision; M.-S.J.: data curation, investigation, methodology, resources, supervision, writing—original draft; C.-F.C.: funding acquisition, investigation, project administration, resources, supervision, writing—original draft, writing—review and editing; Y.-C.T.: data curation, funding acquisition, investigation, methodology, project administration, resources, supervision, writing—original draft, writing—review and editing.

All authors gave final approval for publication and agreed to be held accountable for the work performed therein.

Conflict of interest declaration. We declare we have no competing interests.

Funding. This study was financially supported by the grant from the National Science and Technology Council, Taiwan, Republic of China (MOST 111-2621-M-019-003).

References

1. Dorman DC, Moulin FJ-M, McManus BE, Mahle KC, James RA, Struve MF. 2002 Cytochrome oxidase inhibition induced by acute hydrogen sulfide inhalation: correlation with tissue sulfide concentrations in the rat brain, liver, lung, and nasal epithelium. *Toxicol. Sci.* **65**, 18–25. (doi:10.1093/toxsci/65.1.18)
2. Goffredi S, Childress J, Desaulniers N, Lee R, Lallier F, Hammond D. 1997 Inorganic carbon acquisition by the hydrothermal vent tubeworm *Riftia pachyptila* depends upon high external P_{CO2} and upon proton-equivalent ion transport by the worm. *J. Exp. Biol.* **200**, 883–896. (doi:10.1242/jeb.200.5.883)

3. Hu MY, Guh Y-J, Shao Y-T, Kuan P-L, Chen G-L, Lee J-R, Jeng M-S, Tseng Y-C. 2016 Strong ion regulatory abilities enable the crab *Xenograpsus testudinatus* to inhabit highly acidified marine vent systems. *Front. Physiol* **7**, 14.
4. McMullin ER, Bergquist DC, Fisher CR. 2007 Metazoans in extreme environments: adaptations of hydrothermal vent and hydrocarbon seep fauna. *Gravit. Space Biol. Bull.* **13**, 13–24.
5. Ramirez-Llodra E, Shank TM, German CR. 2007 Biodiversity and biogeography of hydrothermal vent species: thirty years of discovery and investigations. *Oceanography* **20**, 30–41. (doi:10.5670/oceanog.2007.78)
6. Zierenberg RA, Adams MW, Arp AJ. 2000 Life in extreme environments: hydrothermal vents. *Proc. Natl Acad. Sci. USA* **97**, 12 961–12 962. (doi:10.1073/pnas.210395997)
7. Gamenick I, Vismann B, Grieshaber M, Giere O. 1998 Ecophysiological differentiation of *Capitella capitata* (Polychaeta). Sibling species from different sulfidic habitats. *Mar. Ecol. Prog. Ser.* **175**, 155–166. (doi:10.3354/meps175155)
8. Thiermann F, Vismann B, Giere O. 2000 Sulphide tolerance of the marine nematode *Oncholaimus campylocercoides*–a result of internal sulphur formation? *Mar. Ecol. Prog. Ser.* **193**, 251–259. (doi:10.3354/meps193251)
9. Brand GL, Horak RV, Bris NL, Goffredi SK, Carney SL, Govenar B, Yancey PH. 2007 Hypotaurine and thiotaurine as indicators of sulfide exposure in bivalves and vestimentiferans from hydrothermal vents and cold seeps. *Mar. Ecol.* **28**, 208–218. (doi:10.1111/j.1439-0485.2006.00113.x)
10. Yancey PH, Ishikawa J, Meyer B, Girguis PR, Lee RW. 2009 Thiotaurine and hypotaurine contents in hydrothermal-vent polychaetes without thiotrophic endosymbionts: correlation with sulfide exposure. *J. Exp. Zool. A Ecol. Genet. Physiol.* **311**, 439–447. (doi:10.1002/jez.541)
11. Zhang J, Sun QL, Luan ZD, Lian C, Sun L. 2017 Comparative transcriptome analysis of Rimicaris sp. reveals novel molecular features associated with survival in deep-sea hydrothermal vent. *Sci. Rep.* **7**, 1–16. (doi:10.1038/s41598-016-0028-x)
12. Tarasov V, Gebruk A, Mironov A, Moskalev L. 2005 Deep-sea and shallow-water hydrothermal vent communities: two different phenomena? *Chem. Geol.* **224**, 5–39. (doi:10.1016/j.chemgeo.2005.07.021)
13. Han C, Ye Y, Pan Y, Qin H, Wu G, Chen C-TA. 2014 Spatial distribution pattern of seafloor hydrothermal vents to the southeastern Kueishan Tao offshore Taiwan Island. *Acta Oceanol. Sin.* **33**, 37–44. (doi:10.1007/s13131-014-0405-x)
14. Chung SL, Wang SL, Shinjo R, Lee CS, Chen CH. 2000 Initiation of arc magmatism in an embryonic continental rifting zone of the southernmost part of Okinawa Trough. *Terra Nova* **12**, 225–230. (doi:10.1046/j.1365-3121.2000.00298.x)
15. Chen C. 2005 Investigation into extremely acidic hydrothermal fluids off Kueishantao islet, Taiwan. *Acta Oceanol. Sin.* **24**, 125–133.
16. Jeng M-S, Clark PF, Ng PK. 2004 The first zoea, megalopa, and first crab stage of the hydrothermal vent crab *Xenograpsus testudinatus* (Decapoda: Brachyura: Grapsoidea) and the systematic implications for the Varunidae. *J. Crustacean Biol.* **24**, 188–212. (doi:10.1651/C-2359)
17. Ng NK, Huang J, Ho P-H. 2000 Description of a new species of hydrothermal crab, *Xenograpsus testudinatus* (Crustacea: Decapoda: Brachyura: Grapsidae) from Taiwan. *Natl. Taiwan Mus. Publ. Ser.* **10**, 191–199.
18. Jeng MS, Ng NK, Ng PKL. 2004 Feeding behaviour: Hydrothermal vent crabs feast on sea 'snow'. *Nature* **432**, 969. (doi:10.1038/432969a)
19. Vetter R. 1985 Elemental sulfur in the gills of three species of clams containing chemoautotrophic symbiotic bacteria: a possible inorganic energy storage compound. *Mar. Biol.* **88**, 33–42. (doi:10.1007/BF00393041)
20. Yang S-H, Chiang P-W, Hsu T-C, Kao S-J, Tang S-L. 2016 Bacterial community associated with organs of shallow hydrothermal vent crab *Xenograpsus testudinatus* near Kuishan Island, Taiwan. *PLoS ONE* **11**, e0150597. (doi:10.1371/journal.pone.0150597)
21. Pruski A, Médioni AF, Prodon R, Colomines J. 2000 Thiotaurine is a biomarker of sulfide-based symbiosis in deep-sea bivalves. *Limnol. Oceanogr.* **45**, 1860–1867. (doi:10.4319/lo.2000.45.8.1860)
22. Arp A, Childress J, Vetter R. 1987 The sulphide-binding protein in the blood of the vestimentiferan tube-worm, *Riftia pachyptila*, is the extracellular haemoglobin. *J. Exp. Biol.* **128**, 139–158. (doi:10.1242/jeb.128.1.139)
23. Pruski AM, Fiala-Médioni A. 2003 Stimulatory effect of sulphide on thiotaurine synthesis in three hydrothermal-vent species from the East Pacific Rise. *J. Exp. Biol.* **206**, 2923–2930. (doi:10.1242/jeb.00513)
24. Powell M, Somero G. 1985 Sulfide oxidation occurs in the animal tissue of the gutless clam, *Solemya reidi*. *Biol. Bull.* **169**, 164–181. (doi:10.2307/1541396)
25. Leinberger J, Milke F, Christodoulou M, Poehlein A, Caraveo-Patiño J, Teske A, Brinkhoff T. 2022 Microbial epibiotic community of the deep-sea galatheid squat lobster *Munidopsis alvisca*. *Sci. Rep.* **12**, 1–15. (doi:10.1038/s41598-022-06666-x)
26. Vetter R, Wells M, Kurtsman AL, Somero G. 1987 Sulfide detoxification by the hydrothermal vent crab *Bythograea thermydron* and other decapod crustaceans. *Physiol. Zool.* **60**, 121–137. (doi:10.1086/physzool.60.1.30158634)
27. Kelley JL, Arias-Rodriguez L, Patacsil Martin D, Yee M-C, Bustamante CD, Tobler M. 2016 Mechanisms underlying adaptation to life in hydrogen sulfide-rich environments. *Mol. Biol. Evol.* **33**, 1419–1434. (doi:10.1093/molbev/msw020)
28. Menon J, Willsie JK, Tauscher A, Arp AJ. 2003 Epidermal ultrastructure and implications for sulfide tolerance in six species of deep-sea polychaetes. *Invertebr. Biol.* **122**, 334–346. (doi:10.1111/j.1744-7410.2003.tb00098.x)
29. Powell M, Somero G. 1986 Adaptations to sulfide by hydrothermal vent animals: sites and mechanisms of detoxification and metabolism. *Biol. Bull.* **171**, 274–290. (doi:10.2307/1541923)
30. Bright M, Sorgo A. 2003 Ultrastructural reinvestigation of the trophosome in adults of *Riftia pachyptila* (Annelida. Siboglinidae). *Invertebr. Biol.* **122**, 347–368. (doi:10.1111/j.1744-7410.2003.tb00099.x)
31. Cavanaugh CM, Gardiner SL, Jones ML, Jannasch HW, Waterbury JB. 1981 Prokaryotic cells in the hydrothermal vent tube worm *Riftia pachyptila* Jones: possible chemoautotrophic symbionts. *Science* **213**, 340–342. (doi:10.1126/science.213.4505.340)
32. Distel DL, Lee H, Cavanaugh CM. 1995 Intracellular coexistence of methano-and thioautotrophic bacteria in a hydrothermal vent mussel. *Proc. Natl Acad. Sci. USA* **92**, 9598–9602. (doi:10.1073/pnas.92.21.9598)
33. Childress J, Girguis PR. 2011 The metabolic demands of endosymbiotic chemoautotrophic metabolism on host physiological capacities. *J. Exp. Biol.* **214**, 312–325. (doi:10.1242/jeb.049023)
34. Felbeck H, Jarchow J. 1998 Carbon release from purified chemoautotrophic bacterial symbionts of the hydrothermal vent tubeworm *Riftia pachyptila*. *Physiol. Zool.* **71**, 294–302. (doi:10.1086/515931)
35. Chiu L, Wang M-C, Tseng K-Y, Wei C-L, Lin H-T, Yang S-H, Tseng Y-C. 2022 Shallow-water hydrothermal vent system as an extreme proxy for discovery of microbiome significance in a crustacean holobiont. *Front. Mar. Sci.* **9**, 976255. (doi:10.3389/fmars.2022.976255)
36. Goffredi SK. 2010 Indigenous ectosymbiotic bacteria associated with diverse hydrothermal vent invertebrates. *Environ. Microbiol. Rep.* **2**, 479–488. (doi:10.1111/j.1758-2229.2010.00136.x)
37. Hügler M, Petersen JM, Dubilier N, Imhoff JF, Sievert SM. 2011 Pathways of carbon and energy metabolism of the epibiotic community associated with the deep-sea hydrothermal vent shrimp *Rimicaris exoculata*. *PLoS ONE* **6**, e16018. (doi:10.1371/journal.pone.0016018)
38. Ponsard J *et al.* 2013 Inorganic carbon fixation by chemosynthetic ectosymbionts and nutritional transfers to the hydrothermal vent host-shrimp *Rimicaris exoculata*. *ISME J.* **7**, 96. (doi:10.1038/ismej.2012.87)
39. Lallier FH. 1998 Determination of reduced sulfur compounds by high-performance liquid chromatography in hydrothermal seawater and body fluids from Riftia pachyptila. *Analyst* **123**, 1289–1293. (doi:10.1039/a800032h)
40. Laudien J, Schiedek D, Brey T, Pörtner H-O, Arntz W. 2002 Survivorship of juvenile surf clams *Donax serra* (Bivalvia, Donacidae) exposed to severe hypoxia and hydrogen sulphide. *J. Exp. Mar. Biol. Ecol.* **271**, 9–23. (doi:10.1016/S0022-0981(02)00030-8)
41. Goffredi SK, Barry JP. 2002 Species-specific variation in sulfide physiology between closely related Vesicomyid clams. *Mar. Ecol. Prog. Ser.* **225**, 227–238. (doi:10.3354/meps225227)
42. Sahling H, Rickert D, Lee RW, Linke P, Suess E. 2002 Macrofaunal community structure and sulfide flux at

gas hydrate deposits from the Cascadia convergent margin, NE Pacific. *Mar. Ecol. Prog. Ser.* **231**, 121–138. (doi:10.3354/meps231121)

43. Fisher C *et al.* 1988 Physiology, morphology, and biochemical composition of *Riftia pachyptila* at Rose Garden in 1985. *Deep-Sea Res. Pt I* **35**, 1745–1758. (doi:10.1016/0198-0149(88)90047-7)
44. Johnson KS, Childress JJ, Hessler RR, Sakamoto-Arnold CM, Beehler CL. 1988 Chemical and biological interactions in the Rose Garden hydrothermal vent field, Galapagos spreading center. *Deep-Sea Res. Pt I* **35**, 1723–1744. (doi:10.1016/0198-0149(88)90046-5)
45. Zielinski FU, Gennerich HH, Borowski C, Wenzhöfer F, Dubilier N. 2011 In situ measurements of hydrogen sulfide, oxygen, and temperature in diffuse fluids of an ultramafic-hosted hydrothermal vent field (Logatchev, 14°45′N, Mid-Atlantic Ridge): implications for chemosymbiotic bathymodiolin mussels. *Geochem. Geophy. Geosys.* **12**, 1–21. (doi:10.1029/2011GC003632)
46. Butterworth K, Grieshaber M, Taylor A. 2004 Behavioural and physiological responses of the Norway lobster, *Nephrops norvegicus* (Crustacea: Decapoda), to sulphide exposure. *Mar. Biol.* **144**, 1087–1095. (doi:10.1007/s00227-003-1276-4)
47. Jahn A, Gamenick I, Theede H. 1996 Physiological adaptations of *Cyprideis torosa* (Crustacea, Ostracoda) to hydrogen sulphide. *Mar. Ecol. Prog. Ser.* **142**, 215–223. (doi:10.3354/meps142215)
48. Johns A, Taylor A, Atkinson R, Grieshaber M. 1997 Sulphide metabolism in thalassinidean crustacea. *J. Mar. Biol. Assoc. UK* **77**, 127–144. (doi:10.1017/S0025315400033828)
49. Shumway SE, Scott TM, Shick JM. 1983 The effects of anoxia and hydrogen sulphide on survival, activity and metabolic rate in the coot clam, *Mulinia lateralis* (Say). *J. Exp. Mar. Biol. Ecol.* **71**, 135–146. (doi:10.1016/0022-0981(93)90069-Z)
50. Joyner JL, Peyer SM, Lee RW. 2003 Possible roles of sulfur-containing amino acids in a chemoautotrophic bacterium-mollusc symbiosis. *Biol. Bull.* **205**, 331–338. (doi:10.2307/1543296)
51. Achituv Y, Pedrotti M. 1999 Costs and gains of porcelain crab suspension feeding in different flow conditions. *Mar. Ecol. Prog. Ser.* **184**, 161–169. (doi:10.3354/meps184161)
52. Freire CA, Onken H, McNamara JC. 2008 A structure–function analysis of ion transport in crustacean gills and excretory organs. *Comp. Biochem. Physiol. A Mol. Integr. Physiol.* **151**, 272–304. (doi:10.1016/j.cbpa.2007.05.008)
53. Thimgan MS, Berg JS, Stuart AE. 2006 Comparative sequence analysis and tissue localization of members of the SLC6 family of transporters in adult *Drosophila melanogaster*. *J. Exp. Biol.* **209**, 3383–3404. (doi:10.1242/jeb.02328)
54. Nishimura T, Higuchi K, Yoshida Y, Sugita-Fujisawa Y, Kojima K, Sugimoto M, Santo M, Tomi M, Nakashima E. 2018 Hypotaurine is a substrate of GABA transporter family members GAT2/Slc6a13 and TAUT/Slc6a6. *Biol. Pharm. Bull.* **41**, 1523–1529. (doi:10.1248/bpb.b18-00168)
55. Inoue K, Tsukuda K, Koito T, Miyazaki Y, Hosoi M, Kado R, Miyazaki N, Toyohara H. 2008 Possible role of a taurine transporter in the deep-sea mussel *Bathymodiolus septemdierum* in adaptation to hydrothermal vents. *FEBS Lett.* **582**, 1542–1546. (doi:10.1016/j.febslet.2008.03.052)
56. Somero G. 1987 Symbiotic exploitation of hydrogen sulfide. *Physiology* **2**, 3–6. (doi:10.1152/physiologyonline.1987.2.1.3)
57. Jørgensen B. 1982 Ecology of the bacteria of the sulphur cycle with special reference to anoxic-oxic interface environments. *Phil. Trans. R. Soc. Lond. B* **298**, 543–561. (doi:10.1098/rstb.1982.0096)
58. Nelson DC, Jannasch HW. 1983 Chemoautotrophic growth of a marine Beggiatoa in sulfide-gradient cultures. *Arch. Microbiol.* **136**, 262–269. (doi:10.1007/BF00425214)
59. Bagarinao T. 1992 Sulfide as an environmental factor and toxicant: tolerance and adaptations in aquatic organisms. *Aquat. Toxicol.* **24**, 21–62. (doi:10.1016/0166-445X(92)90015-F)
60. Dick GJ, Tebo BM. 2010 Microbial diversity and biogeochemistry of the Guaymas Basin deep-sea hydrothermal plume. *Environ. Microbiol.* **12**, 1334–1347. (doi:10.1111/j.1462-2920.2010.02177.x)
61. Dick GJ. 2019 The microbiomes of deep-sea hydrothermal vents: distributed globally, shaped locally. *Nat. Rev. Microbiol.* **17**, 271–283. (doi:10.1038/s41579-019-0160-2)
62. Faghri MA, Pennington CL, Cronholm LS, Atlas RM. 1984 Bacteria associated with crabs from cold waters with emphasis on the occurrence of potential human pathogens. *Appl. Environ. Microbiol.* **47**, 1054–1061. (doi:10.1128/aem.47.5.1054-1061.1984)
63. Joseph FS, Latha N, Ravichandran S, Devi AS, Sivasubramanian K. 2014 Shell disease in the freshwater crab, *Barytelphusa cunicularis*. *Int. J. Fish Aquat. Stud.* **1**, 105–110.
64. Haditomo A, Prayitno SB. 2018 The bacterial diversity associated with bacterial diseases on Mud Crab (Scylla serrata Fab.) from Pemalang Coast, Indonesia. In *J. Phys. Conf. Ser.*, pp. 012076: IOP Publishing.
65. Meier DV, Pjevac P, Bach W, Hourdez S, Girguis PR, Vidoudez C, Amann R, Meyerdierks A. 2017 Niche partitioning of diverse sulfur-oxidizing bacteria at hydrothermal vents. *ISME J.* **11**, 1545–1558. (doi:10.1038/ismej.2017.37)
66. Halary S, Riou V, Gaill F, Boudier T, Duperron S. 2008 3D FISH for the quantification of methane-and sulphur-oxidizing endosymbionts in bacteriocytes of the hydrothermal vent mussel *Bathymodiolus azoricus*. *ISME J.* **2**, 284–292. (doi:10.1038/ismej.2008.3)
67. Fonseca F, Cerqueira R, Fuentes J. 2019 Impact of ocean acidification on the intestinal microbiota of the marine sea bream (*Sparus aurata* L). *Front. Physiol.* **10**, 1446. (doi:10.3389/fphys.2019.01446)
68. Botté ES, Nielsen S, Abdul Wahab MA, Webster J, Robbins S, Thomas T, Webster NS. 2019 Changes in the metabolic potential of the sponge microbiome under ocean acidification. *Nat. Commun.* **10**, 1–10. (doi:10.1038/s41467-019-12156-y)
69. Chang N-N, Lin L-H, Tu T-H, Jeng M-S, Chikaraishi Y, Wang P-L. 2018 Trophic structure and energy flow in a shallow-water hydrothermal vent: insights from a stable isotope approach. *PLoS ONE* **13**, e0204753. (doi:10.1371/journal.pone.0204753)
70. Weiss MC, Sousa FL, Mrnjavac N, Neukirchen S, Roettger M, Nelson-Sathi S, Martin WF. 2016 The physiology and habitat of the last universal common ancestor. *Nat Microbiol* **1**, 1–8. (doi:10.1038/nmicrobiol.2016.116)
71. Ezenwa VO, Gerardo NM, Inouye DW, Medina M, Xavier JB. 2012 Animal behavior and the microbiome. *Science* **338**, 198–199. (doi:10.1126/science.1227412)
72. Hu MY-A, Hagen W, Jeng M-S, Saborowski R. 2012 Metabolic energy demand and food utilization of the hydrothermal vent crab *Xenograpsus testudinatus* (Crustacea: Brachyura). *Aquat. Biol.* **15**, 11–25. (doi:10.3354/ab00396)
73. Phleger CF, Nelson MM, Groce AK, Cary SC, Coyne K, Gibson JA, Nichols PD. 2005 Lipid biomarkers of deep-sea hydrothermal vent polychaetes—*Alvinella pompejana*, *A. caudata*, *Paralvinella grasslei* and *Hesiolyra bergii*. *Deep-Sea Res. Pt I* **52**, 2333–2352. (doi:10.1016/j.dsr.2005.08.001)
74. Phleger CF, Nelson MM, Groce AK, Cary SC, Coyne KJ, Nichols PD. 2005 Lipid composition of deep-sea hydrothermal vent tubeworm *Riftia pachyptila*, crabs *Munidopsis subsquamosa* and *Bythograea thermydron*, mussels *Bathymodiolus* sp. and limpets *Lepetodrilus* spp. *Comp. Biol. Physiol. B Biochem. Mol. Biol.* **141**, 196–210. (doi:10.1016/j.cbpc.2005.03.001)
75. Chou P-H *et al*. 2023 Cellular mechanisms underlying extraordinary sulfide tolerance in a crustacean holobiont from hydrothermal vents. Figshare. (doi:10.6084/m9.figshare.c.6328044)